

Porphyrin Cosensitization for a Photovoltaic Efficiency of 11.5%: A Record for Non-Ruthenium Solar Cells Based on Iodine Electrolyte

Yongshu Xie,* Yunyu Tang, Wenjun Wu, Yueqiang Wang, Jingchuan Liu, Xin Li, He Tian, and Wei-Hong Zhu*

Key Laboratory for Advanced Materials and Institute of Fine Chemicals, East China University of Science and Technology, Meilong Road 130, Shanghai 200237, People's Republic of China

S Supporting Information

ABSTRACT: Dye-sensitized solar cells (DSSCs) are promising for utilizing solar energy. To achieve high efficiencies, it is vital to synergistically improve the photocurrent (J_{sc}) and the photovoltage (V_{oc}). In this respect, conjugation framework extension and cosensitization are effective for improving the absorption and the J_{sc} , which, however, is usually accompanied by undesirably decreased V_{oc} . Herein, based on a rationally optimized porphyrin dye, we develop a targeted coadsorption/cosensitization approach for systematically improving the V_{oc} from 645 to 727, 746, and 760 mV, with synergistical J_{sc} enhancement from 18.83 to 20.33 mA cm⁻². Thus, the efficiency has been dramatically enhanced to 11.5%, which keeps the record for nonruthenium DSSCs using the I₂/I₃⁻ electrolyte. These results compose an alternative approach for developing highly efficient DSSCs with relatively high V_{oc} using traditional iodine electrolyte.

Increasing energy demand and environmental pollution problems have prompted research on clean and inexhaustive energy sources.¹ In this respect, utilization of solar energy has been demonstrated to be highly promising.² On the basis of traditional silicon-based solar cells, dye-sensitized solar cells (DSSCs) present a promising potential because of their low production cost, easy fabrication, and relatively high solar energy conversion efficiency.³ Since the first report in 1991, increasing interests have been focused on improving the efficiencies of DSSCs.⁴ To this end, it is vital to simultaneously improve the photocurrent (J_{sc}) and the photovoltage (V_{oc}).

Porphyrin dyes have been widely exploited in DSSCs due to their easily modulated structures and strong absorption bands in a wide wavelength range, except the NIR region and around 500 nm.^{5,6} To further improve sunlight harvesting in these two regions, a combined approach of extending the porphyrin conjugation frameworks and application of a cosensitizer is effective for achieving a panchromatic absorption and a high J_{sc} .^{7,8} However, extended conjugation structures may undesirably result in decreased V_{oc} because of aggravated dye aggregation,^{9,10} and cosensitization also usually results in undesirably decreased or nearly unaffected V_{oc} with only a few exceptions.¹¹ Herein, we focus on a systematic cosensitization approach for synergistically improving the V_{oc} and J_{sc} , thus pursuing high efficiencies for DSSCs based on novel extended porphyrin dyes. In virtue of the delicately designed coadsorption/cosensitization, the V_{oc} for

DSSCs based on XW11 (Figure 1) was stepwise improved from 645 to 727, 746, and 760 mV, with a simultaneous J_{sc}

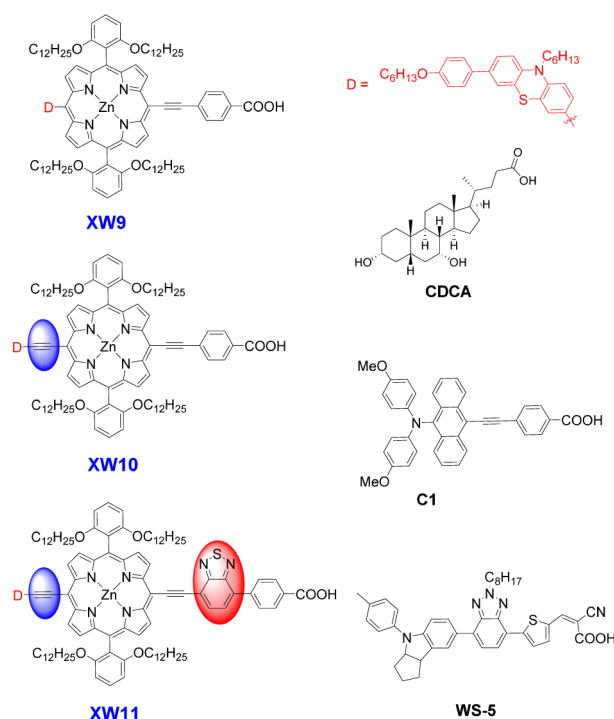


Figure 1. Molecular structures of the porphyrin dyes (XW9, XW10, and XW11), the coadsorbent (CDCA), and the cosensitizers (C1 and WS-5).

enhancement from 18.83 to 20.33 mA cm⁻². As a consequence, the targeted cosensitization can even achieve a photovoltaic efficiency of 11.5%, to the best of our knowledge, a record for nonruthenium DSSCs based on iodine electrolyte.

Sensitizers with strong absorption are highly desirable for improving light harvesting efficiency and J_{sc} . In this regard, porphyrins show a strong Soret band (400–450 nm) and moderate Q-bands (550–600 nm), covering the visible to the near-IR region, with remarkably high molecular absorption coefficients in the visible region (up to 10⁵ M⁻¹ cm⁻¹).^{5,6} The incorporation of conjugated groups can further extend the light

Received: September 21, 2015

Published: October 22, 2015

response range. However, the conjugation extension may induce severe dye aggregation, resulting in a decreased V_{oc} . Thus, all three dyes were specifically wrapped with long alkoxy chains.¹² Furthermore, a phenothiazine moiety was introduced as the electron donor, given its strong electron-donating character and a nonplanar butterfly conformation favorable for further suppressing the aggregation.¹³

As expected, all the dyes feature typical porphyrin absorption spectra with an intense Soret band within 400–480 nm and less intense Q bands within 550–730 nm (Figure 2, Table S1).

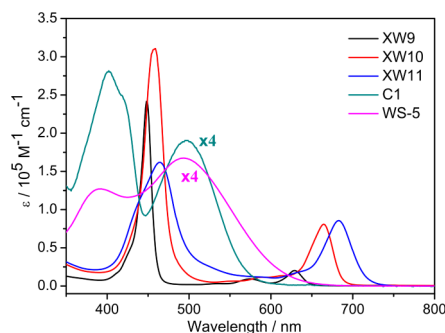


Figure 2. Absorption spectra of dyes XW9, XW10, XW11, C1, and WS-5 in THF.

Compared with XW9, the additional ethynylene bridge and the auxiliary benzothiadiazole group in XW10 and XW11 red-shifted the absorption onset wavelengths from 650 to 700 and 730 nm, respectively, which is favorable for harvesting the sunlight.¹⁴ Furthermore, broadened absorption bands were observed on TiO₂ films (Figure S1) with respect to the corresponding solution spectra, which is also favorable for sunlight harvesting.

The trend of successively red-shifted absorption for XW9, XW10, and XW11 is well consistent with that obtained from the density functional theory (DFT) calculations using the Gaussian 09 program package (Figure S2, Table S2),¹⁵ which also revealed that electron densities of the HOMO orbitals are mainly delocalized over the donor and the porphyrin framework, while the LUMO orbitals are predominantly delocalized over the anchoring group and the porphyrin framework. Thus, the electron transfer from the HOMO to the LUMO can be easily accessible in the electron redistribution from the donor to the anchoring moiety, enabling electron injection from the LUMO to the conduction band of TiO₂. Moreover, suitable HOMO and LUMO energy levels are vital for the electron injection and dye regeneration processes. The HOMOs were obtained to be 0.83, 0.72, and 0.73 V for XW9, XW10, and XW11, respectively, which are more positive than the I₂/I₃⁻ redox potential (0.4 V vs NHE) (Figures S3 and S4, Table S3), and the corresponding LUMO levels were obtained to be -1.12, -1.13, and -1.05 V, respectively, which are more negative than the conduction band edge (CB) of TiO₂ (-0.5 V vs NHE). These results are indicative that both the dye regeneration and electron injection processes are thermodynamically feasible.¹⁶

The porphyrin dyes were evaluated as the sensitizers of DSSCs based on an I₂/I₃⁻ electrolyte. Figure 3 shows the photocurrent–voltage (J – V) curves of the DSSCs measured under simulated AM 1.5G irradiation (100 mW cm⁻²), and the corresponding data are listed in Table 1, with more details listed in Tables S4 and S5. The solar-to-electric power conversion efficiencies (PCE) lie within 7.8–8.6%. As mentioned above, XW9, XW10, and XW11 have successively extended conjugation frameworks

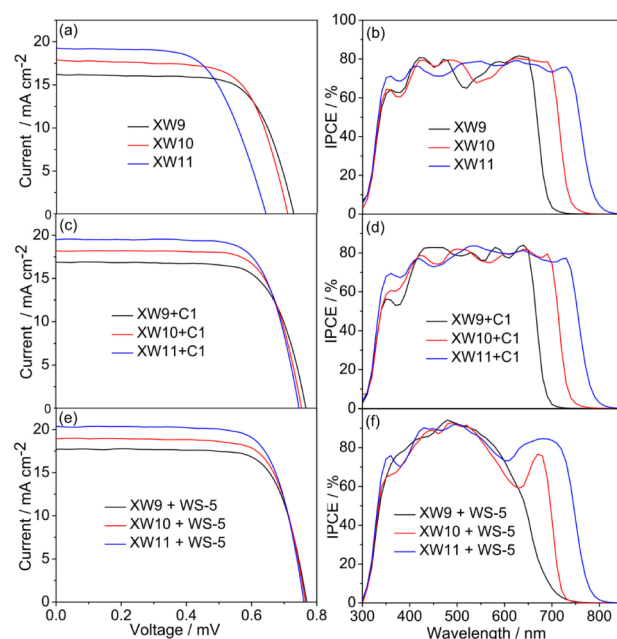


Figure 3. Photocurrent–voltage (J – V) characteristics (a,c,e) and IPCE action spectra (b,d,f) for the DSSCs based on XW9, XW10, and XW11, and cosensitized with C1 or WS-5.

Table 1. Optimized Photovoltaic Data for DSSCs based on XW9, XW10, and XW11 under AM 1.5G Illumination (100 mW cm⁻²)

dyes	J_{sc} (mA cm ⁻²)	V_{oc} (mV)	FF	PCE (%)
XW9	16.27 ± 0.11	728 ± 4	0.698 ± 0.004	8.2 ± 0.1
XW10	17.90 ± 0.04	711 ± 5	0.684 ± 0.005	8.6 ± 0.1
XW11	18.83 ± 0.28	645 ± 3	0.642 ± 0.003	7.8 ± 0.1
XW9 + CDCA	16.17 ± 0.13	740 ± 3	0.689 ± 0.005	8.2 ± 0.1
XW10 + CDCA	17.51 ± 0.17	739 ± 4	0.680 ± 0.005	8.8 ± 0.1
XW11 + CDCA	18.26 ± 0.27	727 ± 2	0.701 ± 0.004	9.3 ± 0.1
XW9 + C1	17.01 ± 0.12	764 ± 2	0.718 ± 0.001	9.3 ± 0.1
XW10 + C1	18.24 ± 0.08	753 ± 4	0.742 ± 0.003	10.1 ± 0.2
XW11 + C1	19.52 ± 0.05	746 ± 5	0.740 ± 0.002	10.6 ± 0.1
XW9 + WS-5	17.70 ± 0.16	770 ± 2	0.741 ± 0.003	10.1 ± 0.1
XW10 + WS-5	19.01 ± 0.11	765 ± 3	0.764 ± 0.004	11.0 ± 0.2
XW11 + WS-5	20.33 ± 0.21	760 ± 4	0.744 ± 0.004	11.5 ± 0.2

and absorption ranges. As a result, they show increasing J_{sc} of 16.27, 17.90, and 18.83 mA cm⁻² (Figure 3a), respectively. Observation of the highest J_{sc} for XW11 is consistent with its broadest absorption. On the other hand, the extended conjugation frameworks brought forth a decreasing V_{oc} of 728, 711, and 645 mV for XW9, XW10, and XW11, respectively, which might be ascribed to the detrimental dye aggregation. As a result of the contradictory trends of J_{sc} and V_{oc} , XW9, XW10, and XW11 demonstrate DSSC efficiencies of 8.2, 8.6, and 7.8%, respectively, with the highest photovoltaic efficiency achieved by XW10. It is also noteworthy that the efficiencies for XW9 and XW10 are higher than those of the corresponding carbazole-based dyes,¹⁷ indicating that the electron-donating effect of phenothiazine is superior to carbazole.

Based on the photovoltaic data, we checked the incident-photon-to-current conversion efficiency (IPCE) action spectra to understand the contribution of absorption at different

wavelengths to the J_{sc} (Figure 3). All the three dyes show a broad IPCE plateau in the visible range. Compared with XW9, the insertion of an ethynylene bridge in XW10 red-shifted the onset wavelength of photocurrent response from 730 to 775 nm, resulting in an increase of J_{sc} from 16.27 to 17.90 mA cm⁻². Further introduction of the benzothiadiazole group in XW11 induced an impressive broad IPCE action spectrum with the onset wavelength red-shifted to 830 nm, resulting in a highest J_{sc} of 18.83 mA cm⁻².

Generally, the utilization of a coadsorbent is effective for suppressing dye aggregation, thus enhancing the V_{oc} . In this respect, chenodeoxycholic acid (CDCA, Figure 1) is the most commonly used due to its nonplanar and bulky configuration.¹⁸ Given the undesirably low V_{oc} values of XW9–XW11, it may be feasible to improve the efficiencies by enhancing the V_{oc} with a coadsorbent. Thus, DSSCs were fabricated by dipping the TiO₂ films into the dye solutions containing CDCA. Upon using 5 mM CDCA, the V_{oc} for XW9, XW10, and XW11 were improved from 728, 711, and 645 mV to 753, 750, and 738 mV, respectively (Tables S6 and S7, Figure S6). Provided that ΔV_{oc} lies in the sequence of XW9 < XW10 < XW11, the suppression of dye aggregation is the most pronounced for XW11 arising from the most serious aggregation due to its largest conjugation framework. Accompanied with the increased V_{oc} , the corresponding J_{sc} values were undesirably decreased to 15.16, 16.47, and 17.17 mA cm⁻², respectively, which is related to the decreased coverage of porphyrin dyes on the TiO₂ films upon coadsorption of CDCA, thus leading to a loss in light harvesting and a decrease in J_{sc} . As a result, the enhancement in photovoltaic efficiency is neglectable for XW9 and XW10. Only XW11 shows a moderate efficiency enhancement from 7.8% to 9.3%, which mainly results from the dramatic enhancement in the V_{oc} .

Although CDCA can be used for improving the V_{oc} by suppressing the dye aggregation, it cannot absorb the sunlight, and thus it does not have photovoltaic effect, which causes decreased J_{sc} and thus is unfavorable for dramatic improving the photovoltaic efficiency. Hence, we continued to delicately design the cosensitization approach for pursuing the synergistic improvement of V_{oc} and J_{sc} . Considering the fact that C1 (Figure 1)¹⁷ demonstrates a broad absorption peak around 500 nm (Figure 2), which well compensates the absorption valley of the porphyrin dyes in this region, we initially used C1 for cosensitization. As expected, the IPCE valleys of the porphyrin dyes around 500 nm were indeed filled up, with the values remaining higher than 75% in this region (Figure 3d,f). As a result, the cosensitized cells show the enhanced J_{sc} values (17.01–19.52 mA cm⁻²) with respect to corresponding individual porphyrin-sensitized cells (Figure 3c, Table 1). More strikingly, the V_{oc} values for XW9, XW10, and XW11 upon cosensitization with C1 were simultaneously improved from 728, 711, and 645 mV to 764, 753, and 746 mV (Table 1), respectively. As we know, a typical cosensitized solar cell usually affords a V_{oc} value between those obtained for the individual dyes.¹⁷ Hence, the cosensitized cells show V_{oc} values between those for individual porphyrin dyes (728–645 mV) and C1 (780 mV). Through successful synergistic enhancement of J_{sc} and V_{oc} , the high photovoltaic efficiencies of 9.3, 10.1, and 10.6% were achieved by cosensitization of C1 with XW9, XW10, and XW11, respectively (Tables 1, S8, and S9).

Based on the successful application of cosensitizer C1, it is anticipated that the efficiencies may be further improved if another matchable cosensitizer with a higher V_{oc} and a higher efficiency is utilized. Thus, we continued to utilize WS-5 as the

alternative cosensitizer, which individually demonstrated a high V_{oc} of 791 mV and a high efficiency of 8.38%.¹⁹ As expected, the V_{oc} values of XW9–XW11 were further improved to 770–760 mV upon cosensitization with WS-5 (Tables 1, S10, and S11). Meanwhile, the IPCE curves showed a high plateau with the maximum reaching as high as 90%, thus achieving high J_{sc} of 17.70–20.33 mA cm⁻² (Figure 3e,f). The 20.33 mA cm⁻² achieved for cosensitization of XW11 with WS-5 (XW11 + WS-5) is slightly higher than the value integrated from the IPCE spectrum (19.80 mA cm⁻², Figure S7). Similar observations have also been reported for a number of porphyrin dyes,²⁰ which may be caused by the more efficient charge transport and collection²¹ as well as stronger thermal effect associated with the full sunlight irradiation.²² As a result, the high photovoltaic efficiencies of 10.1–11.5% were achieved. The excellent photovoltaic behavior of DSSCs based on cosensitization of XW11 with WS-5 was further tested by fabricating a total of 20 cells, which demonstrated good reproducibility (Table S11). Furthermore, one of the cells was also sent to the National Institute of Metrology (NIM), China for certification, and a certified efficiency of 10.9% was obtained (Figure S8). In addition to the high efficiency, the DSSCs also showed satisfactory photostability, with the efficiency remaining at 86% of the initial value after 1000 h of visible-light soaking (Figure S9).

As described above, the V_{oc} values of XW9–XW11 can be systematically improved through cosensitization. Generally, the alteration of the photovoltage originates from a shift of the TiO₂ electron quasi-Fermi-level, which may be ascribed to two major reasons: (i) a shift in the TiO₂ conduction band edge (E_{CB}), which can be inferred from the chemical capacitance (C_{μ}), and (ii) a fluctuation of electron density, which is related to the electron lifetime (τ) determined by the charge recombination rate.^{5a,19} Thus, the electrochemical impedance spectroscopy was checked to obtain the corresponding C_{μ} and τ .

For XW9, the individual porphyrin-based solar cells and the cosensitized ones showed similar C_{μ} values (Figure S10a). Whereas, the corresponding electron lifetimes lie in the order of XW9 < XW9 + C1 < XW9 + WS-5 (Figure S10b), which is indicative of the same order of decreasing charge recombination rates and consistent with the sequence of increasing V_{oc} . These results indicate that the V_{oc} of XW9-based DSSCs are governed by the charge recombination rates. For XW10, the trends for both C_{μ} and τ agree well with that of the V_{oc} values (Figure S10c,d), suggesting that the V_{oc} of XW10-based DSSC may be related to both the charge recombination rates and the positions of the conduction band. Similar to XW9, the V_{oc} values of XW11-based DSSCs are governed by the charge recombination rates (Figure S10e,f).²³

In summary, using a phenothiazine-based electron donor, three porphyrin dyes (XW9–XW11) were rationally designed. Ethynylene and benzothiadiazole (BTD) units were successively introduced to tailor the absorption to longer wavelengths, with the onset wavelengths of photocurrent response red-shifted from 730 nm (XW9) to 830 nm (XW11), which is quite exceptional for organic sensitizers, and thus the corresponding J_{sc} was improved from 16.27 to 18.83 mA cm⁻². However, the V_{oc} value was undesirably decreased from 728 to 645 mV due to the more severe dye aggregation caused by the larger conjugation framework of XW11. To improve the V_{oc} and the photovoltaic efficiency, a delicately designed coadsorption/cosensitization approach was utilized to systematically improve the V_{oc} from 645 to 727, 746, and 760 mV, which was accompanied by synergistically enhanced J_{sc} to 20.33 mA cm⁻². Finally, the

efficiencies for XW11 were successfully improved from 7.8% to 11.5%, which keeps the record for nonruthenium DSSCs using the I_2/I_3^- electrolyte. These results provide further insight into developing efficient DSSCs with synergistically enhanced photovoltage and photocurrent.

■ ASSOCIATED CONTENT

■ Supporting Information

The Supporting Information is available free of charge on the ACS Publications website at DOI: 10.1021/jacs.5b09665.

Synthetic procedures and characterization data of all new compounds; details for all physical characterizations (PDF)

■ AUTHOR INFORMATION

Corresponding Authors

*yshxie@ecust.edu.cn

*whzhu@ecust.edu.cn

Notes

The authors declare no competing financial interest.

■ ACKNOWLEDGMENTS

This work was supported by the Science Fund for Creative Research Groups (21421004), Distinguished Young Scholars (21325625), NSFC/China (21472047, 91227201), and the Oriental Scholarship

■ REFERENCES

- (1) (a) O'Regan, B.; Grätzel, M. *Nature* **1991**, 353, 737. (b) Higashino, T.; Imahori, H. *Dalton Trans.* **2015**, 44, 448. (c) Imahori, H.; Umeyama, T.; Ito, S. *Acc. Chem. Res.* **2009**, 42, 1809.
- (2) (a) Hagfeldt, A.; Boschloo, G.; Sun, L.; Pettersson, H. *Chem. Rev.* **2010**, 110, 6595. (b) Qu, S. Y.; Hua, J. L.; Tian, H. *Sci. China: Chem.* **2012**, 55, 677. (c) Mishra, A.; Fischer, M. K. R.; Bäuerle, P. *Angew. Chem., Int. Ed.* **2009**, 48, 2474. (d) Wu, Y. Z.; Zhu, W. H.; Zakeeruddin, S. M.; Grätzel, M. *ACS Appl. Mater. Interfaces* **2015**, 7, 9307.
- (3) (a) Zhang, S.; Yang, X.; Numata, Y.; Han, L. Y. *Energy Environ. Sci.* **2013**, 6, 1443. (b) Chou, C. C.; Hu, F. C.; Yeh, H. H.; Wu, H. P.; Chi, Y.; Clifford, J. N.; Palomares, E.; Liu, S. H.; Chou, P. T.; Lee, G. H. *Angew. Chem., Int. Ed.* **2014**, 53, 178. (c) Ishida, M.; Hwang, D.; Zhang, Z.; Choi, Y. J.; Oh, J.; Lynch, V. M.; Kim, D. Y.; Sessler, J. L.; Kim, D. *ChemSusChem* **2015**, 8, 2967.
- (4) (a) Wu, Y. Z.; Zhu, W. H. *Chem. Soc. Rev.* **2013**, 42, 2039. (b) Yang, J. B.; Ganesan, P.; Teuscher, J.; Moehl, T.; Kim, Y. J.; Yi, C.; Comte, P.; Pei, K.; Holcombe, T. W.; Nazeeruddin, M. K.; Hua, J. L.; Zakeeruddin, S. M.; Tian, H.; Grätzel, M. *J. Am. Chem. Soc.* **2014**, 136, 5722. (c) Yao, Z. Y.; Zhang, M.; Wu, H.; Yang, L.; Li, R. Z.; Wang, P. *J. Am. Chem. Soc.* **2015**, 137, 3799. (d) Yao, Z. Y.; Zhang, M.; Li, R. Z.; Yang, L.; Qiao, Y. N.; Wang, P. *Angew. Chem., Int. Ed.* **2015**, 54, 5994.
- (5) (a) Li, L. L.; Diau, E. W. G. *Chem. Soc. Rev.* **2013**, 42, 291. (b) Mathew, S.; Yella, A.; Gao, P.; Baker, R. H.; Curchod, B. F. E.; Astani, N. A.; Tavernelli, I.; Rothlisberger, U.; Nazeeruddin, M. K.; Grätzel, M. *Nat. Chem.* **2014**, 6, 242. (c) Higashino, T.; Fujimori, Y.; Sugiura, K.; Tsuji, Y.; Ito, S.; Imahori, H. *Angew. Chem., Int. Ed.* **2015**, 54, 9052. (d) Mai, C. L.; Moehl, T.; Hsieh, C. H.; Décoppet, J. D.; Zakeeruddin, S. M.; Grätzel, M.; Yeh, C. Y. *ACS Appl. Mater. Interfaces* **2015**, 7, 14975.
- (6) Pelleja, L.; Kumar, C. V.; Clifford, J. N.; Palomares, E. *J. Phys. Chem. C* **2014**, 118, 16504.
- (7) (a) Wang, C. L.; Shiu, J. W.; Hsiao, Y. N.; Chao, P. S.; Diau, E. W. G.; Lin, C. Y. *J. Phys. Chem. C* **2014**, 118, 27801. (b) Yao, Z. Y.; Wu, H.; Ren, Y. M.; Guo, Y. C.; Wang, P. *Energy Environ. Sci.* **2015**, 8, 1438.
- (8) Kang, S. H.; Choi, I. T.; Kang, M. S.; Eom, Y. K.; Ju, M. J.; Hong, J. Y.; Kang, H. S.; Kim, H. Y. *J. Mater. Chem. A* **2013**, 1, 3977.
- (9) (a) Joly, D.; Pellejà, L.; Narbey, S.; Oswald, F.; Meyer, T.; Kervella, Y.; Maldivi, P.; Clifford, J. N.; Palomares, E.; Demadrille, R. *Energy*

Environ. Sci. **2015**, 8, 2010. (b) Yan, C. C.; Ma, W. T.; Ren, Y. M.; Zhang, M.; Wang, P. *ACS Appl. Mater. Interfaces* **2015**, 7, 801.

(10) Cabau, L.; Kumar, C. V.; Moncho, A.; Clifford, J. N.; López, N.; Palomares, E. *Energy Environ. Sci.* **2015**, 8, 1368.

(11) Lan, C. M.; Wu, H. P.; Pan, T. Y.; Chang, C. W.; Chen, C. T.; Wang, C. L.; Lin, C. Y.; Diau, E. W. G. *Energy Environ. Sci.* **2012**, 5, 6460.

(12) (a) Sanchis, T. R.; Guo, B. C.; Wu, H. P.; Pan, T. Y.; Lee, H. W.; Raga, S. R.; Santiago, F. F.; Bisquert, J.; Yeh, C. Y.; Diau, E. W. G. *Chem. Commun.* **2012**, 48, 4368. (b) Wang, C. L.; Lan, C. M.; Hong, S. H.; Wang, Y. F.; Pan, T. Y.; Chang, C. W.; Kuo, H. H.; Kuo, M. Y.; Diau, E. W. G.; Lin, C. Y. *Energy Environ. Sci.* **2012**, 5, 6933.

(13) Hua, Y.; Chang, S.; Huang, D. D.; Zhou, X.; Zhu, X. J.; Zhao, J. Z.; Chen, T.; Wong, W. Y.; Wong, W. K. *Chem. Mater.* **2013**, 25, 2146.

(14) Zhu, W. H.; Wu, Y. Z.; Wang, S. T.; Li, W. Q.; Li, X.; Chen, J.; Wang, Z. S.; Tian, H. *Adv. Funct. Mater.* **2011**, 21, 756.

(15) (a) Becke, A. D. *J. Chem. Phys.* **1993**, 98, 5648. (b) Frisch, M. J.; Trucks, G. W.; Schlegel, H. B.; Scuseria, G. E.; Robb, M. A.; Cheeseman, J. R.; Scalmani, G.; Barone, V.; Mennucci, B.; Petersson, G. A.; Nakatsuji, H.; Caricato, M.; Li, X.; Hratchian, H. P.; Izmaylov, A. F.; Bloino, J.; Zheng, G.; Sonnenberg, J. L.; Hada, M.; Ehara, M.; Toyota, K.; Fukuda, R.; Hasegawa, J.; Ishida, M.; Nakajima, T.; Honda, Y.; Kitao, O.; Nakai, H.; Vreven, T.; Montgomery, J. A., Jr.; Peralta, J. E.; Ogliaro, F.; Bearpark, M.; Heyd, J. J.; Brothers, E.; Kudin, K. N.; Staroverov, V. N.; Kobayashi, R.; Normand, J.; Raghavachari, K.; Rendell, A.; Burant, J. C.; Iyengar, S. S.; Tomasi, J.; Cossi, M.; Rega, N.; Millam, N. J.; Klene, M.; Knox, J. E.; Cross, J. B.; Bakken, V.; Adamo, C.; Jaramillo, J.; Gomperts, R.; Stratmann, R. E.; Yazyev, O.; Austin, A. J.; Cammi, R.; Pomelli, C.; Ochterski, J. W.; Martin, R. L.; Morokuma, K.; Zakrzewski, V. G.; Voth, G. A.; Salvador, P.; Dannenberg, J. J.; Dapprich, S.; Daniels, A. D.; Farkas, Ö.; Foresman, J. B.; Ortiz, J. V.; Cioslowski, J.; Fox, D. J. *Gaussian 09, Revision A.2*, Gaussian, Inc.: Wallingford, CT, 2009.

(16) Hagberg, D. P.; Yum, J. H.; Lee, H.; Angelis, F. D.; Marinado, T.; Karlsson, K. M.; Baker, R. H.; Sun, L. C.; Hagfeldt, A.; Grätzel, M.; Nazeeruddin, M. K. *J. Am. Chem. Soc.* **2008**, 130, 6259.

(17) (a) Wang, Y. Q.; Chen, B.; Wu, W. J.; Li, X.; Zhu, W. H.; Tian, H.; Xie, Y. S. *Angew. Chem., Int. Ed.* **2014**, 53, 10779. (b) Li, Z.; Li, Q. Q. *Sci. China: Chem.* **2014**, 57, 1491. (c) Wei, T. T.; Sun, X.; Li, X.; Ågren, H.; Xie, Y. S. *ACS Appl. Mater. Interfaces* **2015**, 7, 21956.

(18) (a) Mikroyannidis, J. A.; Suresh, P.; Roy, M. S.; Sharma, G. D. *Electrochim. Acta* **2011**, 56, S616. (b) Lim, J.; Kwon, Y. S.; Park, T. *Chem. Commun.* **2011**, 47, 4147.

(19) Li, W. Q.; Wu, Y. Z.; Zhang, Q.; Tian, H.; Zhu, W. H. *ACS Appl. Mater. Interfaces* **2012**, 4, 1822.

(20) (a) Wu, H. P.; Qu, Z. W.; Pan, T. Y.; Lan, C. M.; Huang, W. K.; Lee, H. W.; Reddy, N. M.; Chen, C. T.; Chao, W. S.; Yeh, C. Y.; Diau, E. W. G. *Energy Environ. Sci.* **2012**, 5, 9843. (b) Chang, S.; Wang, H. D.; Hua, Y.; Li, Q.; Xiao, X. D.; Wong, W. K.; Wong, W. Y.; Zhu, X. J.; Chen, T. *J. Mater. Chem. A* **2013**, 1, 11553.

(21) Frank, A. L.; Kopidakis, N.; Lagemaat, J. *Coord. Chem. Rev.* **2004**, 248, 1165.

(22) Cao, Y. M.; Bai, Y.; Yu, Q. J.; Cheng, Y. M.; Liu, S.; Shi, D.; Gao, F. F.; Wang, P. *J. Phys. Chem. C* **2009**, 113, 6290.

(23) (a) Yella, A.; Lee, H. W.; Tsao, H. N.; Yi, C. Y.; Chandiran, A. K.; Nazeeruddin, M. K.; Diau, E. W. G.; Yeh, C. Y.; Zakeeruddin, S. M.; Grätzel, M. *Science* **2011**, 334, 629. (b) Hardin, B. E.; Snaith, H. J.; McGehee, M. D. *Nat. Photonics* **2012**, 6, 162.